STUDY OF ALPHA-GAMMA CORRELATION IN THE REACTION PLANE AND THE MECHANISM OF THE $^{28}Si(\alpha, \alpha'\gamma)\,^{28}Si^*$ REACTION

By K. Bodek, A. Budzanowski, L. Jarczyk, R. Kulessa, J. Majewski, A. Strzałkowski, W. Waluś and G. Willim

Institute of Physics, Jagellonian University, Cracow*

and

Institute of Nuclear Physics, Cracow**

(Received March 9, 1982)

The alpha-gamma correlations have been measured between the α-particles inelastically scattered to the 1.78, 4.62, 4.98, 6.28, 7.38 and 7.80 MeV excited states in ^{28}Si and the gamma rays corresponding to the first excited–ground state transition. The incident α-particle energies were 24, 26, 27 and 27.5 MeV. The analysis of the correlation functions and inelastic scattering cross-sections were performed in terms of the statistical and direct reaction models. Hauser-Feshbach, Coupled Channels and DWBA type of calculations were carried out and conclusions concerning reaction mechanism are given.

PACS numbers: 25.60.-t, 25.60.Cy

1. Introduction

Elastic and inelastic scattering in the alpha plus ^{28}Si system exhibits complicated features: e.g. strong fluctuations in excitation functions, backward angles enhancement of the differential cross section [1]. It is expected that these features reflect the competition between various reaction mechanisms. Usual procedure to determine contributions of different type of reaction processes based on the analysis of experimental cross section only leads to ambiguous results.

It is to be expected that experimental data on the alpha-gamma correlations should provide more information which can help to understand the reaction mechanism as these data contain information on the polarization of the final nucleus state. The alpha-gamma

* Address: Instytut Fizyki, Uniwersytet Jagielloński, Reymonta 4, 30-059 Kraków, Poland.
** Address: Instytut Fizyki Jądrowej, Radzikowskiego 152, 31-342 Kraków, Poland.

correlation for the first excited state of ^{28}Si was measured at 21.5 MeV by Blatchley et al. [2]. They have analysed data assuming pure direct mechanism with the aim to find out the best fit optical model potential. At low energies the alpha-gamma coincidence cross sections for ^{28}Si(α, $\alpha'\gamma$) ^{28}Si* measured by Prasad et al. [3] were analysed in terms of the Hauser-Feshbach model.

The aim of the present work is to study the angular correlation between the different alpha particle groups corresponding to low lying excited states of the ^{28}Si nucleus and the gamma transition between the first excited 1.78 MeV (2^+) and the ground state at the incident energy sufficiently high where the competition between various reaction mechanisms will be clearly visible.

2. *Experimental procedure and results*

The alpha-gamma correlation functions were measured with the alpha particles with the energies 24, 26, 27 and 27.5 MeV from the U-120 cyclotron of the Institute of Nuclear Physics in Cracow. The beam with intensity 60 nA was collimated to the spot with diameter 3 mm on the self supporting silicon target of the thickness 150 μg/cm^2. Fig. 1 shows the lay-out of the measuring system. A silicon surface barrier detector located in the scattering

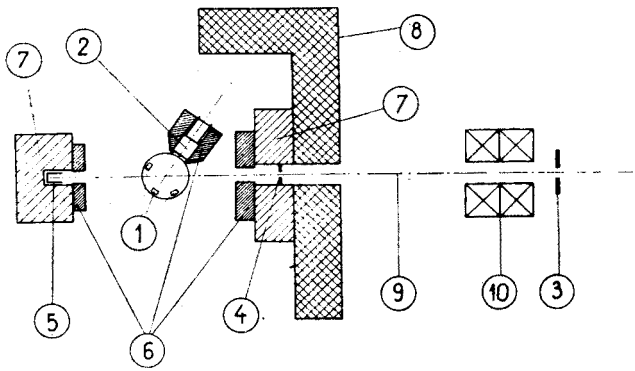

Fig. 1. The lay-out of the experimental arrangement. *1* — particle detectors, *2*— gamma detector, *3* —tantalum slit 10×10 mm, *4* — bismuth slit, *5* — Faraday cup, *6* — lead shielding, *7* — poliethylene-boron shielding, *8* — barite concrete shielding, *9* — beam axis, *10* — quadrupole lenses

chamber was used to detect alpha particles. The separation of alpha particles from protons was achieved by controlling the depletion depth of the detector. A rectangular slit 3 mm × 8 mm placed in front of the detector determined the angular resolution ±2 deg. Gamma rays were detected with a 3″ × 3″ 12S8/E-O Harshaw NaI(Tl) scintillation detector located outside the chamber. Its angular resolution was ±12 deg. The range of angles accessible to the gamma detector was from 40 to 140 deg. In order to reduce the gamma background a special attention was paid to the beam guiding system. The details of the collimation and shielding are shown in Fig. 1.

The alpha-gamma coincidences were handled in the typical "fast-slow" system presented diagrammatically in Fig. 2. The memory routing system enabled to register in the

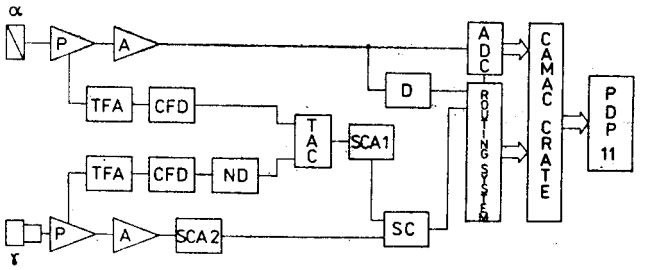

Fig. 2. Block diagram of the electronics. P — preamplifier, A — linear amplifier, TFA — timing filter amplifier, CFD — constant fraction discriminator, ND — nanosecond delay, TAC — time to amplitude converter, SCA — single channel analyser, SC — slow coincidence system, ADC — analog to digital converter

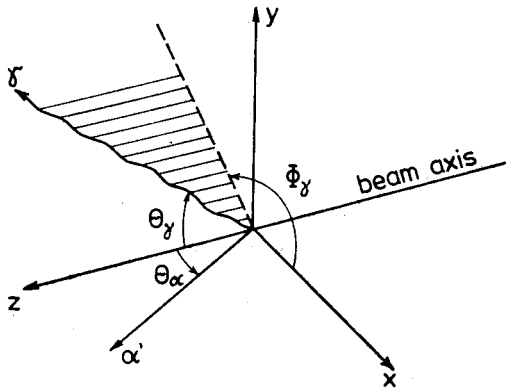

Fig. 3. Definition of the α-particle and γ ray angles

memory of the PDP 11/10 computer simultaneously both single and coincidence spectra. The measurements were performed in the reaction plane. Definitions of angles are presented in Fig. 3.

Correlation functions were measured between alpha groups corresponding to the 1.78(2^+), 4.62(4^+), 4.98(0^+), 6.28(3^+), 7.38(2^+) and 7.80(3^+) states and the gamma line corresponding to the transition between 1.78(2^+) first excited and the ground state. The measurements were performed for eight alpha particle scattering angles: θ_{LAB} = 27.5, 40.0, 46.0, 65.0, 157.5, 159.0, 162.5 and 165.0 deg. The gamma detection angle was changed from 40 to 140 deg in 10 deg steps. The typical single and coincident spectra are shown in Fig. 4.

The normalized correlation functions were calculated from the measured number of coincidences N_C corrected for the random coincidences and the number of counts in the corresponding peaks in single spectra N using the formula

$$W = \frac{4\pi}{\varepsilon_\gamma \Delta\Omega_\gamma} \cdot \frac{N_C}{N}, \qquad (1)$$

where ε_γ and $\Delta\Omega_\gamma$ denote the efficiency and solid angle of the gamma detector. The factor $4\pi/\varepsilon_\gamma\Delta\Omega_\gamma$ was determined from the measurement of the correlation function of the

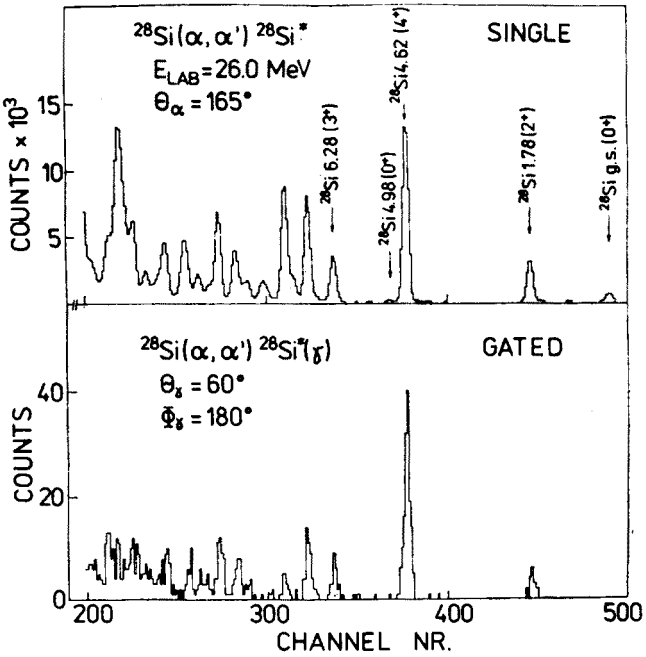

Fig. 4. Single and gated by 1.78 MeV γ line α-particle spectra

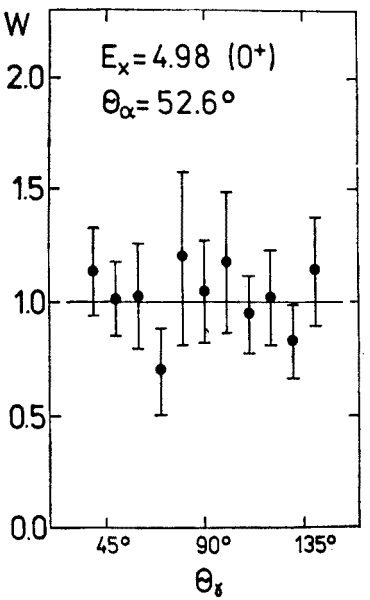

Fig. 5. The measured correlation function for the 4.976(0$^+$) state

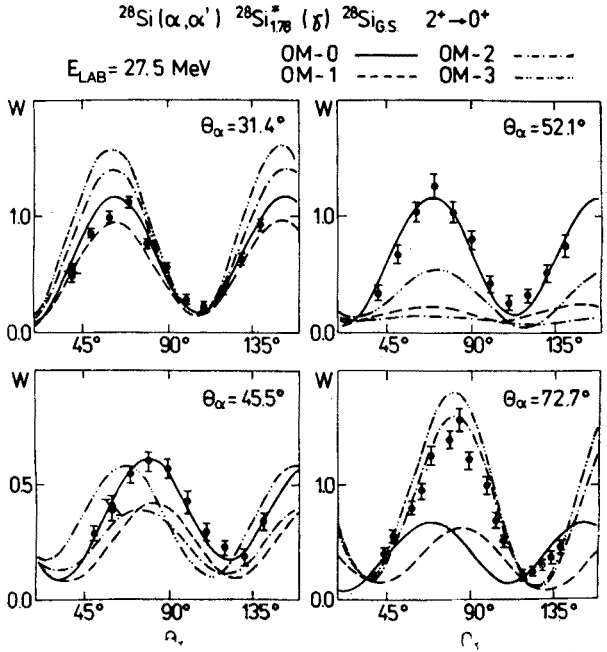

Fig. 6

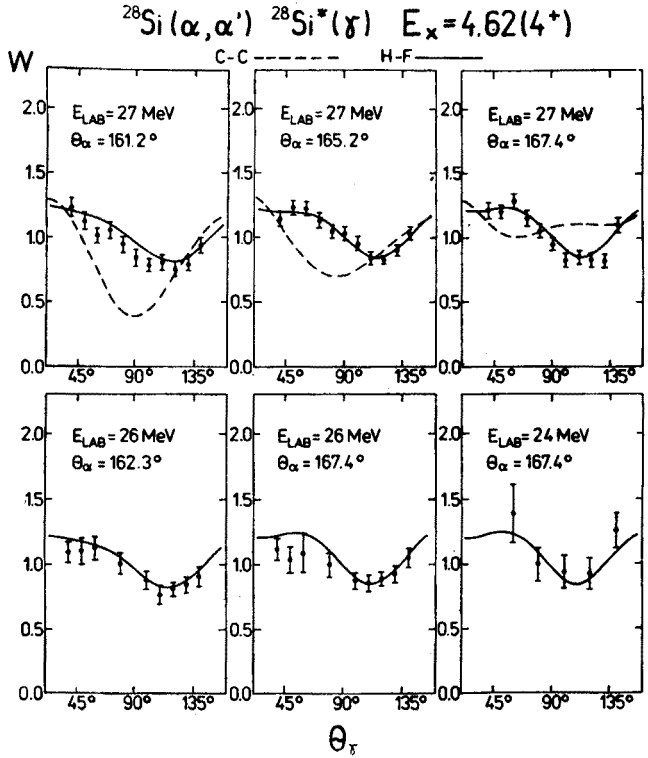

Fig. 7

Fig. 6. The correlation function between the α-particles inelastically scattered to the first excited 1.78(2^{+}) state and the γ quanta from the 1.78(2^{+}) to the ground state transition in ^{28}Si for different α-emission angles. Solid, dashed, dot-dashed and double dot dashed lines indicate the DWBA fits using different O. M. parameter sets of increasing depth of the real part respectively

Fig. 7. The correlation function between α-particles inelastically scattered to the 4.62(4^{+}) state and γ-quanta from the 1.78(2^{+}) to the ground state transition in ^{28}Si. Solid and dashed line indicate results of the Hauser-Feshbach and Coupled-Channels models calculations respectively

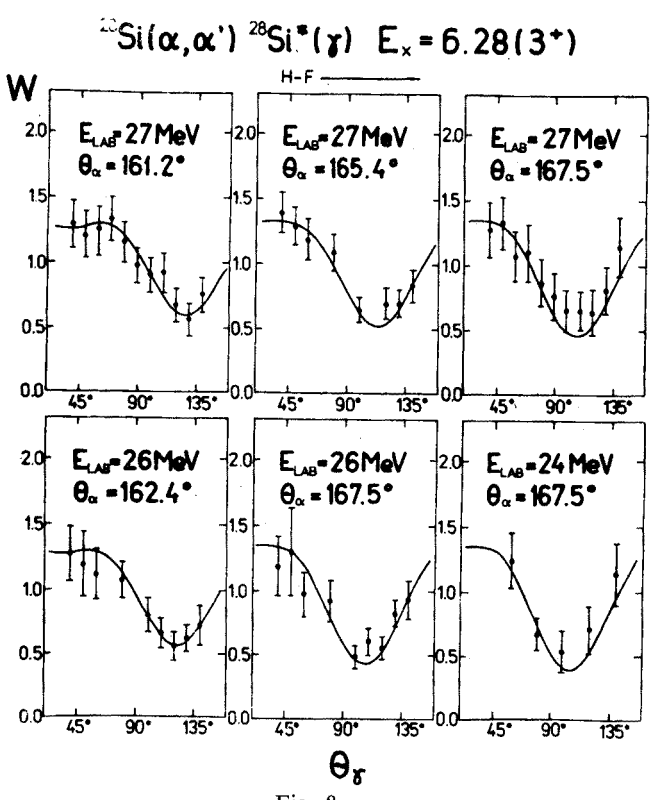

Fig. 8

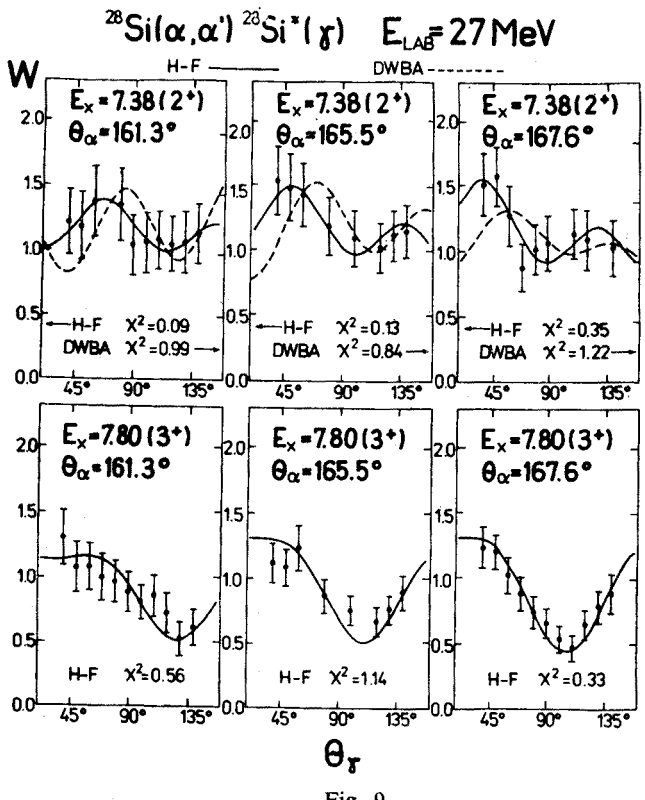

Fig. 9

Fig. 8. The correlation function between α-particles inelastically scattered to the 6.28(3+) state and γ-quanta from the 1.78(2+) to the ground state transition in ^{28}Si. Solid line indicates results of the Hauser-Feshbach model calculation

Fig. 9. The correlation functions between α-particles inelastically scattered to the 7.38(2+) and 7.80(3+) excited states and γ-quanta from the 1.78(2+) to the ground state transition in ^{28}Si. Solid and dashed lines indicate results of the Hauser-Feshbach and DWBA models calculations respectively

1.78 MeV gamma line with alpha particles corresponding to the 4.98(0^+) level, see Fig. 5. Since the spin of this level is zero the correlation function is isotropic and equals 1.

The obtained correlation functions for six excited states of ^{28}Si are presented in Figs. 5–9. The correlation functions for the 7.38(2^+) and 7.80(3^+) states are not normalized

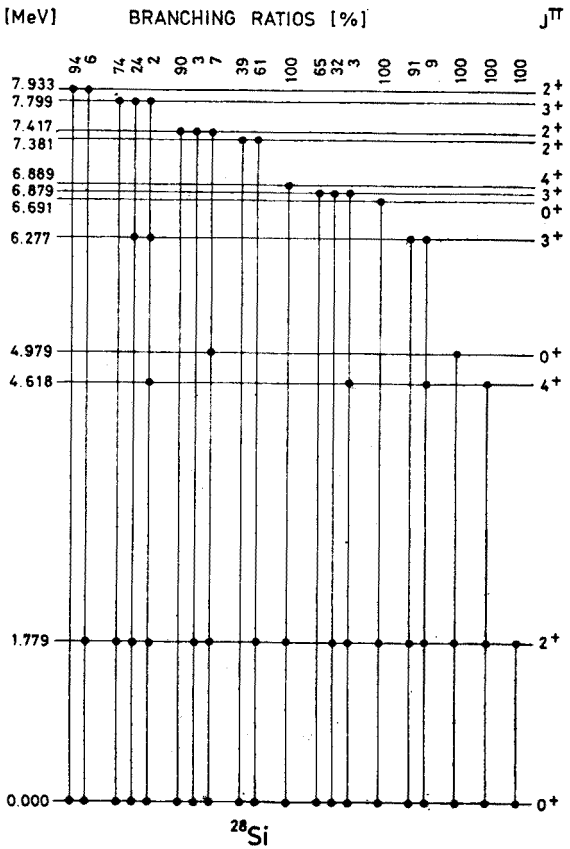

Fig. 10. Decay scheme of the low lying excited states in ^{28}Si

because the corresponding peaks overlap in single spectra with those of 7.42(2^+) and 7.93(2^+), respectively. These last two states are only weakly contributing to the coincidence spectra owing to the branching ratios which favorize 7.38(2^+) and 7.79(3^+) states (Fig. 10).

3. *Analysis*

The angular distributions and angular correlation functions were analysed under assumption that two reaction mechanisms contribute incoherently to the reaction. According to this the measured single and double differential cross section can be expressed as follows

$$\frac{d\sigma^{D+HF}}{d\Omega_\alpha} = \frac{d\sigma^{D}}{d\Omega_\alpha} + \frac{d\sigma^{HF}}{d\Omega_\alpha}$$

and

$$\frac{d^2\sigma^{D+HF}}{d\Omega_\alpha d\Omega_\gamma} = \frac{d^2\sigma^{D}}{d\Omega_\alpha d\Omega_\gamma} + \frac{d^2\sigma^{HF}}{d\Omega_\alpha d\Omega_\gamma}, \tag{2}$$

where D and HF denote direct and Hauser-Feshbach contributions to the cross section. As the gamma decay of the residual nucleus is independent of the way of its formation we can express the double differential cross section in the form [4]

$$\frac{d^2\sigma}{d\Omega_\alpha d\Omega_\gamma} = \frac{1}{4\pi}\frac{d\sigma}{d\Omega_\alpha}(\theta_\alpha) W(\theta_\alpha, \theta_\gamma, \phi_\gamma).$$

Thus the second equation in (2) can be rewritten as

$$\left[\frac{d\sigma^{D}}{d\Omega_\alpha} + \frac{d\sigma^{HF}}{d\Omega_\alpha}\right] W^{D+HF} = \frac{\sigma^{D}}{d\Omega_\alpha} W^{D} + \frac{d\sigma^{HF}}{d\Omega_\alpha} W^{HF}$$

and finally

$$W^{D+HF} = \left[\frac{d\sigma^{D}}{d\Omega_\alpha} W^{D} + \frac{d\sigma^{HF}}{d\Omega_\alpha} W^{HF}\right] \Big/ \left[\frac{d\sigma^{D}}{d\Omega_\alpha} + \frac{d\sigma^{HF}}{d\Omega_\alpha}\right],$$

where W^{D+HF} denotes the correlation function which is to be compared with the experimental one.

The correlation function can be written as a sum [4]:

$$W(\theta_\alpha, \theta_\gamma, \phi_\gamma) = \sum_{kq} t_{kq}(\theta_\alpha) T^*_{kq}(\theta_\gamma, \phi_\gamma)$$

where the statistical tensor t_{kq} describes the polarization of the final nucleus and is predicted by various reaction models. For the direct reaction mechanism t^{D}_{kq} were calculated according to [5]. In order to obtain t^{HF}_{kq} for the compound reaction mechanism compatible to those of DWBA model we have written

$$t^{HF}_{kq}(\theta_\alpha) = t'_{kq}(\theta_\alpha)/t'_{00}(\theta_\alpha),$$

where

$$t'_{kq}(\theta_\alpha) = \sum (-1)^{J_A - J + j_b + s_a - s_b - q} \sqrt{\frac{(\nu-q)!}{(\nu+q)!}}$$

$$\times (2l_a+1)(2j_a+1)(2J+1)^2(2l_b+1)(2j_b+1)(2\mu+1)^{1/2}(2\nu+1)^{1/2}$$

$$\times \langle l_a l_a 00|\mu 0\rangle W(l_a l_a j_a j_a; \mu s_a) W(j_a j_a J J; \mu J_A)$$

$$\times \langle l_b l_b 00|\nu 0\rangle W(l_b l_b j_b j_b; \nu s_b) \langle \mu\nu 00|kq\rangle$$

$$\times \begin{pmatrix} J & J & \mu \\ j_b & j_b & \nu \\ J_B & J_B & k \end{pmatrix} T_{l_a j_a}(E_a) T_{l_b j_b}(E_b) G^{-1}(J\pi E_x) P^q_\nu(\cos\theta_\alpha).$$

The sum extends over $l_a, j_a, l_b, j_b, J, \pi, \mu$ and ν. (s_a, l_a, j_a) and (s_b, l_b, j_b) denote the spin, orbital and total angular momentum of the incoming and outgoing particle, respectively, whereas (J, π) are the spin and parity of the compound system. J_A and J_B denote spins of the target and residual nucleus, respectively. $T_{l_a j_a}(E_a)$ and $T_{l_b j_b}(E_b)$ are the transmission coefficients in the initial and final channels, respectively. $G(J\pi E_x)$ — so called Hauser-Feshbach denominator — is a sum of transmission coefficients over all open channels of decay of the compound system with a spin J and parity π at the excitation energy E_x.

The efficiency tensor T_{kq} depends only on the properties of the gamma transition [6]. A more detailed description of calculation of the T_{kq} is given in the Appendix I.

The direct part of the cross section for the excitation of the 1.78(2^+) state was calculated in terms of the DWBA model using VENUS code [5] which allows also to calculate statistical tensors. Since the transition to the 4.62(4^+) state involves two-phonon excitation a coupled channels program JUPITOR-1 [7] was used. For the purpose of the angular correlation analysis this program was modified in a way which enabled to calculate statistical tensors. A specially written program PIOTR [8] provided the Hauser-Feshbach differential cross section and statistical tensors as well. The T_{kq} efficiency tensor was calculated with the CORDE [9] program which evaluated also the final correlation function.

The optical model parameters necessary for the DWBA and HF calculations were obtained from the analysis of the elastic scattering data. For the purpose of the present investigation we have chosen data from Refs. [10], [11]. Performed analysis led to several

TABLE I

Optical potential parameters for ^{28}Si

Set. no.	V_0 [MeV]	V_1	W_0 [MeV]	W_1	r_0 [fm]	a [fm]
OM -0-	47.24	−0.845	2.676	0.215	1.791	0.520
OM -1-	75.45	−0.879	3.653	0.214	1.664	0.564
OM -2-	107.11	−0.818	5.612	0.199	1.589	0.560
OM -3-	147.46	−0.880	7.367	0.192	1.533	0.551

sets of best fit optical model parameters listed in Table I. From the point of view of the elastic scattering data analysis these parameter sets were considered as equivalent ones. It was found that the results of the Hauser-Feshbach calculations are insensitive to the choice of different sets of the OM parameters.

An excitation of rotational type was assumed for the direct part of the cross section. According to systematics given by Siemaszko [12] we have used the following values for the quadrupole and hexadecapole deformation parameters: $\beta_2 = -0.30$, $\beta_4 = +0.08$.

The parameters necessary for the Hauser-Feshbach model calculation were chosen using the procedure described elsewhere [13].

The T_{kq} efficiency tensors were calculated using parameters from Ref. [14]. The comparison of the calculated cross section and correlation functions with measured ones are presented in Figs. 5–9.

4. Discussion

a) Transition to the first excited 1.78(2^+) state

In Figs. 11 and 6 the angular distribution and correlation functions for the inelastic scattering to the first excited 1.78(2^+) state calculated in DWBA model with different optical model potentials from Table I are shown. As can be seen only the shallow potential

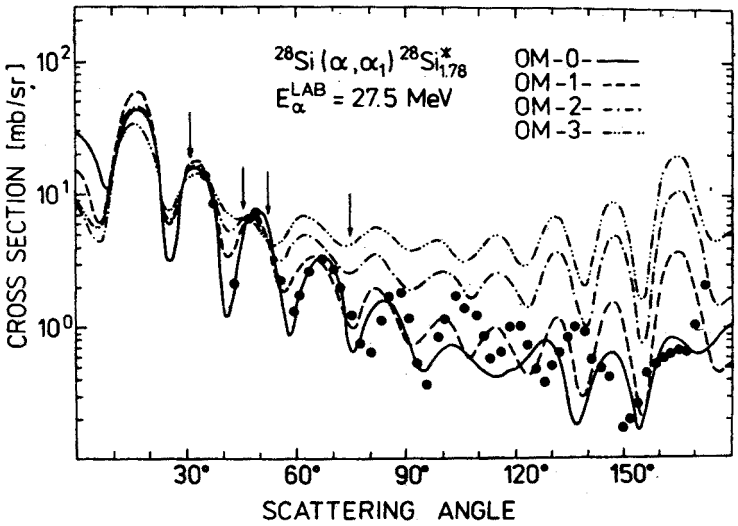

Fig. 11. Experimental and calculated cross sections for the inelastic α-scattering to the first excited 1.78(2^+) state of ^{28}Si. The solid, dashed, dot-dashed and double dot-dashed lines indicate results of the DWBA model calculations using different optical model potentials with the increasing depth of the real potential well respectively. Arrows indicate angles at which the correlation functions were measured

gives reasonable fits to the cross section and correlation functions for forward angles. The deep potential following from folding models [15] or suggested from fits at higher energies led to evidently inferior reproduction of the data. In order to understand this somewhat contradictory property of the optical model potentials we have examined the contributions to the overlap integrals of various partial waves in the incoming channel. It turned out that (see Fig. 12) deep potentials give too large transition probability for partial waves with small orbital angular momenta thus the reaction loses its surface character. We then concluded that deep potentials are not suitable for DWBA calculations at low energies. Further analysis was done using the shallow family potential discussed above. At angles of alpha particle emission smaller than 70 deg both the cross section and correlation function are well fitted using pure direct mechanism, however at larger scattering angles discrepancies can be noticed. They are especially pronounced for the correlation function. Inclusion of the contribution from the compound nucleus calculated in the Hauser-Feshbach model improves considerably the fits (see Figs 13, 14). The fits for the 1.78(2^+) state were repeated using the coupled channel theory. It was found that coupled

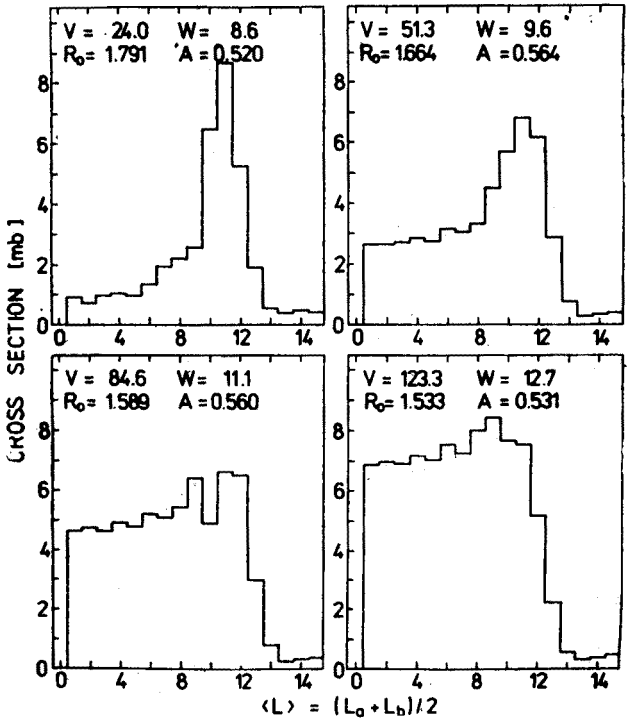

Fig. 12

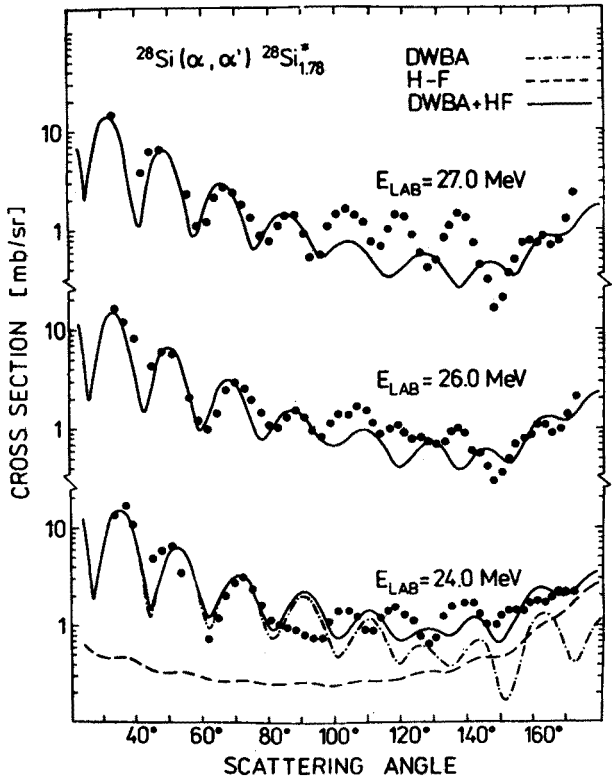

Fig. 13

Fig. 12. Contributions to the angle integrated cross sections for the inelastic α-scattering to the first excited 1.78(2^+) state in ^{28}Si from different partial waves L_a and L_b in the incident and outgoing channels respectively, calculated in terms of the DWBA model using different sets of the optical potential parameters as indicated

Fig. 13. Differential cross section for the inelastic scattering of α-particles to the 1.78(2^+) excited state in ^{28}Si at various incident α-particle energies. The calculated incoherent sum of the direct process (DWBA model) and compound process (Hauser-Feshbach model) is indicated by a solid line. The dashed and dot-dashed lines represent results of the Hauser-Feshbach and DWBA models respectively

channel calculations with 0^+-2^+-4^+ coupling did not introduce essential changes in the quality of fits resulting only in 10 percent reduction of the imaginary part of the optical model potential.

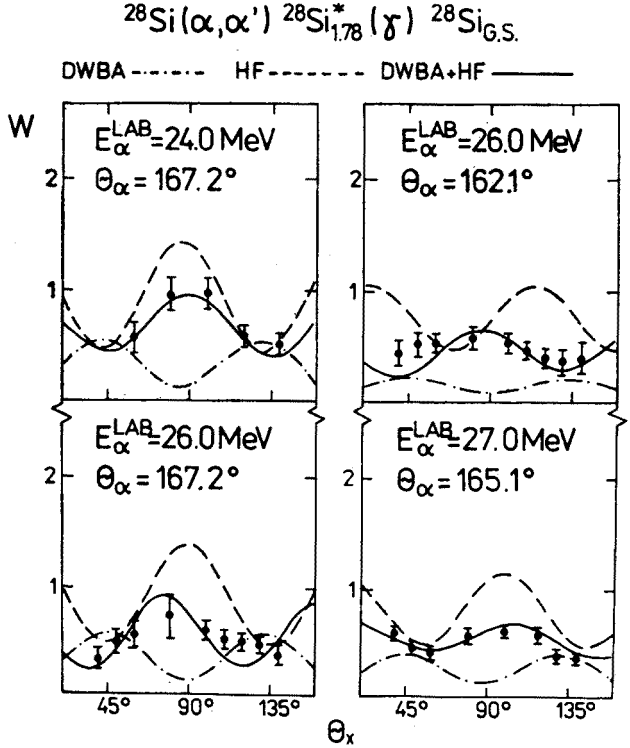

Fig. 14. Correlation function between the alpha particles inelastically scattered to the 1.78(2^+) state and γ-quanta corresponding to the first excited-ground state transition in ^{28}Si. Solid line represents result of Hauser-Feshbach + DWBA calculations. Dot-dashed and dashed lines represent results of the calculations assuming pure direct (DWBA) or pure compound (HF) models of reaction

b) Transition to the 4.62(4^+) state

Since the known β_4 value is rather small the only way to excite the 4.62(4^+) state in a direct process is through a two phonon transition. Therefore we performed a series of coupled channel calculations. Although a magnitude and average shape of the angular distribution could be reproduced, it was impossible to obtain within this model the agreement with the experimental correlation function. This curve could be well reproduced assuming the pure compound nucleus mechanism. However in this case the calculated absolute value of the cross section is lower than experimental one. The sum of the direct cross section (with slightly adjusted β_2 value) and compound nucleus contribution can give reasonable fits to the cross section both in shape and magnitude, however the agreement with angular correlation curve is evidently worse than for pure compound nucleus process. Extensive analysis in terms of the coupled channel theory in which the deformation

and optical model parameters were varied did not improve fits to the angular correlation curves. We conclude then that the transition to the 4.62(4^+) state cannot be described in terms of a pure collective model.

c) Transition to the 6.28(3^+), 7.38(2^+) and 7.80(3^+) states

In the energy range under investigation the direct cross section decreases strongly with increasing excitation energy. Additionally the direct one-phonon transition to the unnatural parity states is strictly forbidden in the case of 0^+-0^+ target-projectile system. Therefore we confined our analysis for the 6.28(3^+), 7.38(2^+) and 7.80(3^+) states to the compound mechanism only. As can be seen from Figs 8 and 9 good fits to the correlation functions were obtained.

In conclusion we can say that studies of the correlation function can clearly distinguish various reaction mechanisms. At the energies considered in present investigation the transition to the lowest 2^+ state of ^{28}Si is dominated by single phonon direct excitation process, while the transitions for states above 6 MeV are well described by pure compound nucleus model. Calculations indicate that in case of transition to the 4.62(4^+) state the direct and compound processes contribute significantly to the cross section. However a comparison of the results of calculations with measured correlation functions strongly suggests the domination of the compound nucleus mechanism.

APPENDIX

Gamma decay efficiency tensor

The gamma radiation accompanying deexcitation of a polarized state is a good tool to measure this polarization. The detailed method how to calculate the efficiency tensor of gamma transition was described by Brink and Rose [6]. Here we write only some final

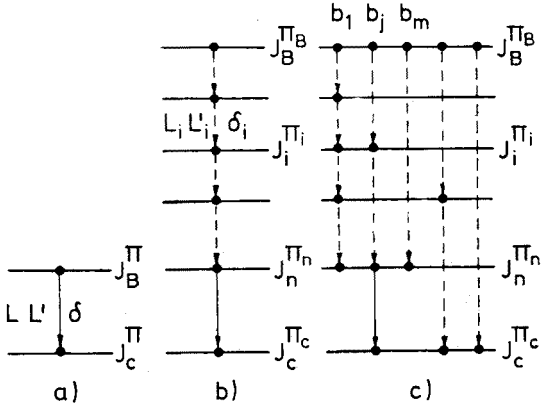

Fig. 15. Various possibilities for calculating the gamma efficiency tensor: a) one decay, b) one cascade with last transition detected, c) branched cascade with last transition detected

formulas which were coded in the CORDE computer program. There are three basic cases which are schematically represented in Fig. 15: a) single transition, b) gamma cascade where only the last transition is observed, c) branched gamma cascade where several branches go through the last observed transition.

a) Let the initial polarized state with defined spin J_B and parity π_B decay into the final state with spin J_C and parity π_C in a single gamma transition (Fig. 15a). The efficiency tensor of such transition may be written as a product

$$T_{kq}(\theta_\gamma, \phi_\gamma) = A_k(J_B, J_C) C_{kq}(\theta_\gamma, \phi_\gamma),$$

where $\theta_\gamma, \phi_\gamma$ denote polar angles describing the direction of the gamma ray, C_{kq} is the renormalized spherical harmonic

$$C_{kq}(\theta_\gamma, \phi_\gamma) = \sqrt{\frac{4\pi}{2k+1}}\, Y_k^q(\theta_\gamma, \phi_\gamma)$$

and

$$A_k(J_B, J_C) = \frac{1}{1+\delta^2}\{R_k(L, L) + 2\delta R_k(L, L') + \delta^2 R_k(L', L')\},$$

where

$$R_k(L, L') = (-1)^{1+J_B-J_C+L'-L-k}\sqrt{(2J_B+1)(2L+1)(2L'+1)}$$
$$\times \langle LL'1-1|k0\rangle W(J_B J_C LL'; kJ_C).$$

$\langle LL'1-1|k0\rangle$ denotes a Clebsch-Gordan coefficient and $W(J_B J_C LL'; kJ_C)$ is a Racah coefficient. δ denotes a mixing ratio defined according to the phase convention from Ref. [6]. L is the lowest angular momentum carried out by the radiation and $L' = L+1$. k and q fulfil inequalities $0 \leqslant k \leqslant 2J_B$ and $-k \leqslant q \leqslant +k$, respectively. If we do not observe the polarization of the gamma radiation the A_k vanish for odd values of k.

b) Let the initial state $(J_B\pi_B)$ decay into the final one $(J_C\pi_C)$ through the gamma cascade and only the last transition $(J_n\pi_n) \to (J_C\pi_C)$ is observed (Fig. 15b). Each unobserved transition introduces into the efficiency tensor the depolarization factor U_k, so that

$$T_{kq}(\theta_\gamma, \phi_\gamma) = A_k(J_n, J_C) \prod_{i=1}^{n} U_k(J_{i-1}J_i) C_{kq}(\theta_\gamma, \phi_\gamma),$$

where

$$U_k(J_{i-1}J_i) = (-1)^k \frac{1}{1+\delta_i^2}\left\{\begin{matrix} W(J_{i-1}J_iJ_{i-1}J_i; L_ik) \\ W(J_{i-1}J_iJ_{i-1}J_i; L_i0) \end{matrix}\right.$$
$$\left. + \delta_i^2 \frac{W(J_{i-1}J_iJ_{i-1}J_i; L_i'k)}{W(J_{i-1}J_iJ_{i-1}J_i; L_i'0)}\right\}.$$

Unobserved transitions may reduce the maximal rank of the efficiency tensor: $0 \leqslant k \leqslant 2 \times \min(J_B, J_1, \ldots, J_n)$.

c) For the situation shown in Fig. 15c where m branches with branching ratios b_j lead to the observed transition, the efficiency tensor is a bit more complicated

$$T_{kq}(\theta_\gamma, \phi_\gamma) = A_k(J_n, J_C) \frac{\sum_{j=1}^{m} b_j \prod_{i=1}^{n} u_k(J_{i-1}^j J_i^j)}{\sum_{j=1}^{m} b_j} C_{kq}(\theta_\gamma, \phi_\gamma).$$

Taking into account a finite size of the gamma detector leads to the so called attenuation factors f_k in the efficiency tensor. Method of calculation of f_k is described in Ref. [4]. In Table II we have collected values of the efficiency tensor for gamma transitions in the ^{28}Si considered in the present work. We define T_k as a product of the A_k, U_k and f_k coefficients.

TABLE II

Gamma decay efficiency tensor for low lying states of ^{28}Si nucleus

Excit. energy [MeV]	Spin parity	Observed transition	T_0	T_2	T_4
1.78	2^+	1.78 g.s.	1.0000	−0.5765	−0.9467
4.62	4^+	1.78 g.s.	1.0000	−0.4319	−0.2695
4.98	0^+	1.78 g.s.	1.0000	—	—
6.28	3^+	1.78 g.s.	1.0000	−0.4649	−0.3634
7.38	2^+	1.78 g.s.	0.6100	−0.1758	0.3850
7.80	3^+	1.78 g.s.	1.0000	−0.4451	−0.3092

REFERENCES

[1] A. Budzanowski, L. Jarczyk, B. Kamys, A. Kapuścik, *Nucl. Phys.* **A265**, 461 (1976).
[2] D. E. Blatchley, R. D. Bent, *Nucl. Phys.* **61**, 641 (1965).
[3] R. Prasad, A. Hofmann, F. Vogler, *Nucl. Phys.* **A255**, 64 (1975).
[4] F. Rybicki, T. Tamura, G. R. Satchler, *Nucl. Phys.* **A146**, 659 (1970).
[5] T. Tamura, W. H. Coker, F. Rybicki, *Comp. Phys. Com.* **2**, 92 (1971).
[6] H. J. Rose, D. H. Brink, *Rev. Mod. Phys.* **39**, 306 (1967).
[7] T. Tamura, *Rev. Mod. Phys.* **37**, 679 (1965); Oak Ridge National Laboratory, Report No. 4152 (unpublished).
[8] K. Bodek (unpublished).
[9] K. Bodek (unpublished).
[10] A. W. Obst, K. W. Kemper, *Phys. Rev.* **C6**, 1705 (1972).
[11] A. Bobrowska, A. Budzanowski, K. Grotowski, L. Jarczyk, B. Kamys, S. Micek, H. Polok, A. Strzałkowski, Z. Wróbel, *Acta Phys. Pol.* **B3**, 533 (1972).
[12] H. Siemaszko, thesis (unpublished).
[13] L. Jarczyk, M. Siemaszko, Silesian Univ. Report No. 270, Katowice 1979.
[14] P. M. Endt, C. Van der Leun, *Nucl. Phys.* **A214**, 1 (1973).
[15] A. Budzanowski, A. Dudek, K. Grotowski, Z. Majka, A. Strzałkowski, *Part. Nucl.* **6**, 97 (1973).